IEEE TRANSACTIONS ON

BIOMEDICAL ENGINEERING

A PUBLICATION OF THE IEEE ENGINEERING IN MEDICINE AND BIOLOGY SOCIETY

Indexed in PubMed® and MEDLINE®, products of the United States National Library of Medicine

MARCH 2011 VOLUME 58 NUMBER 3 IEBEAX (ISSN 0018-9294)

PART II OF TWO PARTS

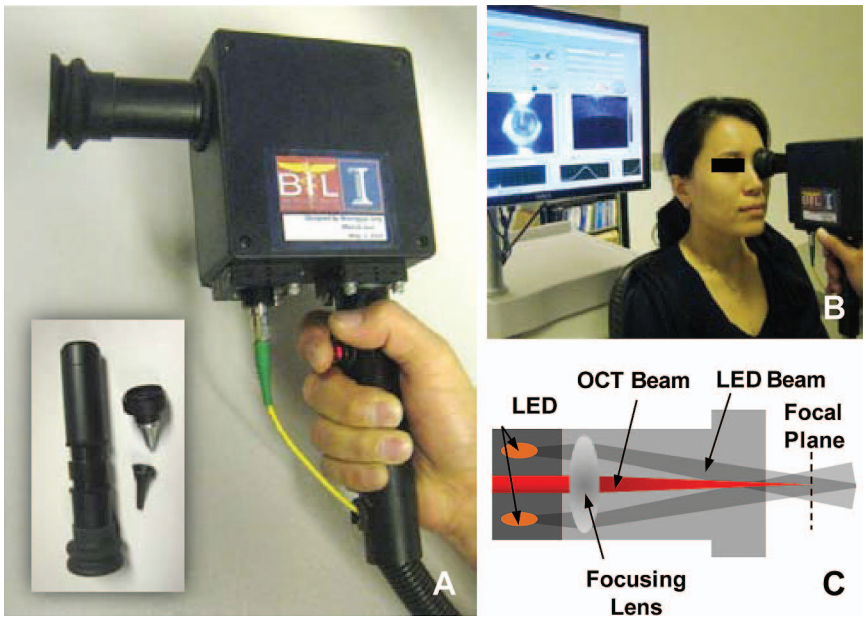

(a) Photographs of handheld OCT scanner and lens mounts. All lens mounts were packaged in threaded lens tubes for convenient interchange. (b) Photograph of OCT imaging procedure. Physician positions handheld scanner on tissue, orients to the desired imaging location, and clicks a save button mounted on the scanner handle while monitoring both video and OCT images. (c) Schematic of optical paths for the OCT and LED beams in the lens mount. Two red LEDs are permanently mounted in the handheld scanner for video imaging. The lens in the interchangeable tube guides and focuses the OCT beam as well as the LED beams to scan and uniformly illuminate the tissue. As shown in "Handheld Optical Coherence Tomography Scanner for Primary Care Diagnostics" by Jung *et al.*, p. 742.

Handheld Optical Coherence Tomography Scanner for Primary Care Diagnostics

Woonggyu Jung, Jeehyun Kim, Mansik Jeon, Eric J. Chaney, Charles N. Stewart, and Stephen A. Boppart*, *Fellow, IEEE*

***Abstract*—The goal of this study is to develop an advanced point-of-care diagnostic instrument for use in a primary care office using handheld optical coherence tomography (OCT). This system has the potential to enable earlier detection of diseases and accurate image-based diagnostics. Our system was designed to be compact, portable, user-friendly, and fast, making it well suited for the primary care office setting. The unique feature of our system is a versatile handheld OCT imaging scanner which consists of a pair of computer-controlled galvanometer-mounted mirrors, interchangeable lens mounts, and miniaturized video camera. This handheld scanner has the capability to guide the physician in real time for finding suspicious regions to be imaged by OCT. In order to evaluate the performance and use of the handheld OCT scanner, the anterior chamber of a rat eye and *in vivo* human retina, cornea, skin, and tympanic membrane were imaged. Based on this feasibility study, we believe that this new type of handheld OCT device and system has the potential to be an efficient point-of-care imaging tool in primary care medicine.**

***Index Terms*—Handheld imaging scanner, optical coherence tomography (OCT), primary care medicine.**

I. Introduction

PRIMARY care is the medical specialty that offers most patients their first contact with the health care system. A primary care physician typically encounters and diagnoses a wide variety of diseases and illnesses, requiring a broad knowledge base in many areas of medicine. Primary care physicians initially collect information about the present symptoms and signs, past medical history, and other health details from the patient and conduct a physical examination. Despite technological advances in many other areas of medicine and surgery, primary care physicians still use somewhat historical methods that rely on keen observations and comprehensive knowledge to diagnose illness and monitor a patient's condition. These qualitative diagnostics based on symptoms and signs can frequently be a cause of misdiagnosis in less common or new cases of disease.

As medical imaging technology has advanced over the last few decades, imaging has been primarily used for the detection and diagnosis of diseases in tissue. It permits the acquisition, visualization, and analysis of new types of diagnostic data that can further improve the outcome of the patient visit. However, most available imaging modalities such as MRI, CT, plain-film X-ray, and ultrasound imaging have significant constraints that make them impractical to adapt to the primary care setting. Two ubiquitous diagnostic imaging tools in the primary care office are the otoscope and ophthalmoscope, which offer magnified visualization and access to the ear canal and tympanic membrane, as well as the anterior chamber and retina of the eye, respectively. However, these simple optical devices are only able to image the surface morphology of tissues, and are unable to image subsurface features which may be of significant diagnostic value. Due to this current lack of advanced diagnostic imaging instruments in primary care offices, there is a great need to develop new visual and quantitative methods to improve the diagnostic outcome of the patient visit, to assist the physician in reaching the correct diagnosis, and to ensure appropriate patient referral to subspecialists, particularly in a cost-conscious healthcare system.

Optical coherence tomography (OCT) is a cross-sectional imaging method based on the detection of backscattered near infrared light from tissue [1]. It is capable of noninvasive, high-resolution imaging in real time. The miniaturization of OCT beam delivery systems with optical fiber and micro optics in endoscopes and catheters [2], [3], microscopes [4], needle-probes [5], and handheld scanners [6], [7], is another advantage. These characteristics of OCT are well suited for imaging in the primary care clinical setting because OCT meets the requirements for diagnostics in limited time and space. In addition, laboratory-based OCT and large commercial OCT systems have been extensively used to image the eye [8], [9], skin [10], and oral cavity [11], [12], which are some of the more common tissue sites examined by the primary care physician. In fact, to date, ophthalmic imaging has become the largest clinical application for OCT. However, no OCT technology or research has been specifically targeted for primary care medicine, despite a clear need.

In this letter, we report a new handheld OCT scanner and system as a high resolution, fast, and convenient diagnostic

Manuscript received July 21, 2010; revised October 6, 2010; accepted November 21, 2010. Date of publication December 3, 2010; date of current version February 18, 2011. This work was supported in part by research grants from the National Institutes of Health (NIBIB, R01 EB005221 and NCI, R21/R33 CA115536, S.A.B.), Blue Highway, LLC, Syracuse, NY, and Welch Allyn, Inc., Skaneateles Falls, NY. *Asterisk indicates corresponding author.*

W. Jung and E. J. Chaney are with the Beckman Institute for Advanced Science and Technology, Urbana, IL 61801 USA (e-mail: wgjung@illinois.edu; echaney@illinois.edu).

J. Kim and M. Jeon are with the School of Electronics Engineering, Kyungpook National University, Daegu 702-701, Korea (e-mail: jeehk@knu.ac.kr; freesoul@ee.knu.ac.kr).

C. N. Stewart is with Blue Highway, LLC, Syracuse, NY 13244-4100 USA, and also with Welch Allyn, Inc., Skaneateles Falls, NY 13152 USA (e-mail: cstewart@blue-highway.com).

*S. A. Boppart is with the Departments of Electrical and Computer Engineering, Bioengineering, and Internal Medicine, University of Illinois at Urbana-Champaign, Urbana, IL 61801 USA (e-mail: boppart@illinois.edu).

Color versions of one or more of the figures in this paper are available online at http://ieeexplore.ieee.org.

Digital Object Identifier 10.1109/TBME.2010.2096816

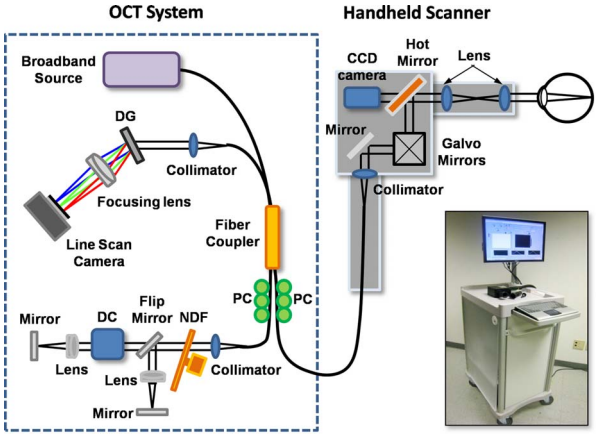

Fig. 1. Schematic and photograph of the cart-based SD-OCT system and handheld scanner. The optical setup, including the spectrometer and reference optical path, is contained within a small portable medical cart. The handheld scanner has a 2 m-long connecting cable with optical fiber and electrical wires, so that the physician can readily access multiple tissue sites on the patient. *Abbreviations:* DG, diffraction grating; PC, polarization controller; DC, dispersion compensation materials; NDF, neutral density filter.

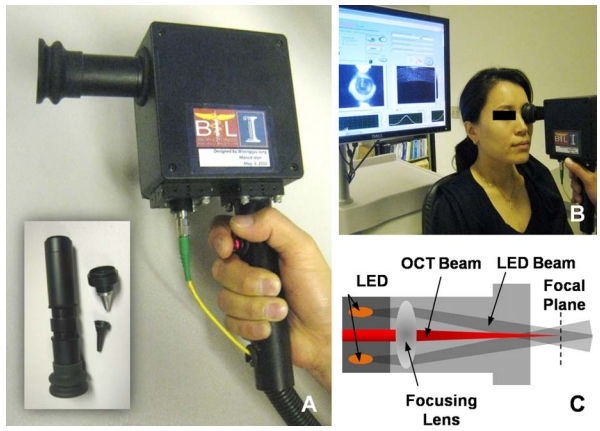

Fig. 2. (a) Photographs of handheld OCT scanner and lens mounts. All lens mounts were packaged in threaded lens tubes for convenient interchange. (b) Photograph of OCT imaging procedure. Physician positions handheld scanner on tissue, orients to the desired imaging location, and clicks a save button mounted on the scanner handle while monitoring both video and OCT images. (c) Schematic of optical paths for the OCT and LED beams in the lens mount. Two red LEDs are permanently mounted in the handheld scanner for video imaging. The lens in the interchangeable tube guides and focuses the OCT beam as well as the LED beams to scan and uniformly illuminate the tissue.

instrument for primary care. This technology enables one to visualize not only the surface of the various tissues, but also cross-sectional structure using the high speed OCT imaging technology. Therefore, it offers the potential for more accurate and detailed feedback for quantitative diagnosis, and provides digital 2-D or 3-D datasets that can be used in diagnostic decision making, or can be shared with other clinical providers involved in the care of the patient. We tested the performance of our system by imaging *in vivo* human and rat tissues.

II. Materials and Methods

A. Compact and Portable OCT System

Our OCT system was specifically designed for the unique clinical environment of a primary care office. Since a typical primary care setting has limited available space and the physician needs to rapidly acquire data to reach a diagnosis, an OCT system must be compact in size and should have the capability of high-speed imaging. Fig. 1 shows a schematic and photograph of the cart-based spectral domain OCT (SD-OCT) system that was developed in this study. The portable medical cart (66 cm depth $\times$ 50 cm width $\times$ 94 cm height) contained all the optical hardware including light source, handheld OCT imaging scanner, computer, and computer monitor.

Our SD-OCT system has a fiber optic Michelson interferometer configuration which has four ports. The light from a superluminescent diode (Superlum) source, having a 70-nm full-width-half-maximum spectral bandwidth at the center wavelength of 830 nm providing $\sim$4 μm axial resolution in tissue, was guided into one port of the 2 $\times$ 2 fiber coupler, and split into reference and sample arms. In the sample arm, a versatile handheld scanner was implemented with a 2-m long optical fiber and electrical wire. Our handheld OCT scanner utilizes a pair of galvanometer-mounted mirrors and interchangeable lens mounts for imaging different tissue sites. The lens mounts were designed and optimized to image the cornea, retina, tympanic membrane, mouth, and the skin. Depending on the focusing optics, the transverse resolution of the system was $\sim$15 μm. In the reference arm, two different optical paths were constructed, a long optical path length was used for retinal imaging while a short path was used for imaging other tissues. The reference path for retinal imaging also contained a dispersion compensation unit to account for the dispersion within the optics of the human eye and the handheld scanner. Reference paths were switched by way of a flip mirror. The reflected signals from each arm are recombined at the 2 $\times$ 2 fiber coupler and the resulting spectral interference is captured by a custom designed spectrometer. The spectrometer consists of a collimator, transmittance grating with 1200 lines/mm (Wasatch Photonics), achromatic doublet lens, and CMOS line scan camera (Basler) with 2048 pixels and a line scan acquisition rate of 140 kHz. Spectral data from the line scan camera of the spectrometer are then digitized by a frame grabber (National Instruments), sampled, and rescaled as a function of the wave number, and finally visualized after image processing. Data were acquired and processed at 70 422 axial scans per second, or an image rate of $\sim$70 frames/s with each image having 1000 axial scans (columns) of data.

B. Handheld OCT Scanner

All the optics in the handheld scanner were packaged inside a light and robust plastic box (11.5 cm $\times$ 11.5 cm $\times$ 6.3 cm) as shown in Fig. 2(a). Three different lens mounts for imaging the retina, ear, and other tissues were designed to conform to the outer shape of the ear and eye and to provide ready comfortable access to tissue in real time. In particular, the ear lens mount was constructed by modifying the same metal ear tip used in existing commercial otoscopes. This allowed for the use of disposable ear specula for each patient. All lens mounts were housed in a 1-in threaded lens tube. The focal lengths of the lenses were optimized for the position where the scanner was in

contact with the tissues, as shown in Fig. 2(b). In our scanner, a miniature (charge-coupled device) CCD-based color video camera having a size of 1.6 cm (diameter) $\times$ 2.1 cm (length) and 0.27 megapixel was integrated for capturing video images of tissue surface features during acquisition of OCT images. This camera was essential for precise positioning of the OCT beam over small suspicious areas, and provided digital video documentation correlating surface features with depth-resolved OCT imaging.

In order to illuminate the imaging site for CCD-based video imaging, two red LEDs were used that were located immediately behind the focusing lens, as shown in Fig. 2(c). This configuration avoids the back-reflection of LED light from the focusing lens, and provides a uniform illumination across the imaging site by the focusing lens. Electrical wires powering the LEDs were connected to the analog outputs of the data acquisition (DAQ) board in the computer, and the operations module for the LEDs was integrated within the existing imaging software so that the on/off and brightness levels of the LEDs could be adjusted by the user with the computer. Physicians can also operate the system and save OCT and video images using button controls mounted on the scanner handle. These functions help the primary care physician to direct the OCT beam to the specific regions of tissue or suspicious sites in real time, and without requiring any additional personnel assistance to operate the system.

C. Enhancement of Imaging Speed

SD-OCT is based on a wavelength-resolved detection scheme. The modulated spectrum detected by the line scan camera contains information that is used to infer the location of reflections from tissue sites in depth, along the sampling beam.

One of the drawbacks of SD-OCT is the broadening of the point-spread function with increasing depth, when a linear relationship between the wave number and the pixel position is not maintained. Therefore, precise spectral calibration is required for obtaining accurate biological tissue cross-sectional images. Various methods have been introduced for this linear calibration [13]–[15]. Software-based methods are relatively common because they provide a convenient calibration procedure [16]. However, software-based methods are computationally very intensive, which significantly decreases the imaging speed.

In this study, we used a novel linear calibration method that offers a sufficient number of sampling points and does not require any computation. This method uses a translating-slit-based wavelength filter to acquire information on the wavelength-pixel position. The wavelength-swept spectra are coregistered with the pixel positions, which can be automatically measured with a camera and an optical spectrum analyzer. Since this calibration method is a one-time procedure, it does not require a filter or a software recalibration algorithm during OCT imaging. Currently, our software is based on Visual C++ having a multithreading structure. It takes advantages of parallel-data processing and system control, allowing efficient data communication. Therefore, both the calibration method and multithread structure that were used in this study increases the imaging speed by reducing the computational load.

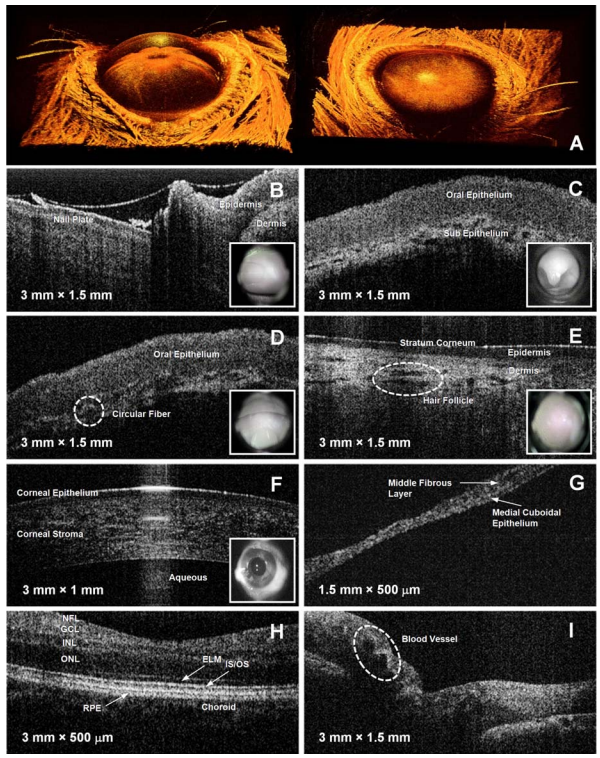

Fig. 3. *In vitro* 3-D OCT images of a rat eye (a) and *in vivo* OCT and video images acquired from normal human tissue (b–i). (a) Reconstructed 3-D OCT images of anterior chamber of a rat eye at angled view (left) and a top view (right), (b) fingernail plate and fold, (c) uvula, (d) oral mucosa along gumline, (e) skin on arm, (f) cornea, (g) tympanic membrane in ear, (h) foveal region of retina, and (i) optic nerve head. *Abbreviations:* NFL, nerve fiber layer; GCL, ganglion cell layer; INL, inner nuclear layer; ONL, outer nuclear layer; ELM, external limiting membrane; IS/OS, junction between the inner and outer segment of the photoreceptors; RPE, retinal pigment epithelium.

III. Results

Under protocols approved by the Institutional Review Board and the Institutional Animal Care and Use Committee at the University of Illinois at Urbana-Champaign, real-time 2-D and 3-D OCT images were acquired from a rat eye and normal human volunteers as shown in Fig. 3. Fig. 3(a) shows the reconstructed 3-D anterior chamber image of the rat eye from a top view and an angled view. For 3-D imaging, sequential 2-D images (B-scans) were continuously saved and displayed in real time during scanning. The size of the acquired 3-D volume was 10 mm $\times$ 10 mm $\times$ 1.5 mm, with 2048 axial sampled points in depth along each A-scan, and with each cross-sectional B-scan composed of 1000 A-scans or columns of data. In both images, eye structures such as the cornea, iris, and even thin hairs, are clearly identified. We also found detailed structural information by extracting 2-D OCT images from this 3-D data set at various locations. Fig. 3(b)–(i) shows OCT images and corresponding video images of various *in vivo* human tissues that visualize detailed tissue morphology.

The lens mount for imaging the oral cavity included a cover glass to protect the optics from contamination. The distance from the lens mount to the focal plane was 2.5 cm, which was sufficient to image back to the uvula. For ear imaging, an ear

piece [see Fig. 2(a)] having a 2-mm exit aperture was used, which determined the size of the OCT image in the lateral direction, as seen in Fig. 3(g). A soft eyecup was attached to the lens mount for imaging both the anterior and posterior chambers of eye. This not only provided comfortable contact for the human subject, but also matched the focal length of the eye and provided flexibility for angular positioning. Currently, this handheld scanner does not provide CCD-based video images of the ear and the posterior chamber of the eye because the focus of the camera lens and the magnification of the camera are fixed by the optics within the scanner. However, video imaging at all sites is possible by varying the camera optics. The current field of view of the camera is limited to 10°, providing a 2-cm video image at the focal plane of OCT beam. The center of the video image was aligned with the lateral scanning path of the OCT beam as seen in Fig. 3(b)–(f). Thus, the video image helps to determine and direct the precise location of a suspicious region in the tissue that a primary care physician may wish to image with OCT in real time [17]–[19]. In addition, the physician can readily make direct comparisons between the OCT and video images because both images are co-registered in both space and time, and digitally stored together. Thus, the entire imaging procedure using this handheld OCT scanner is straightforward and convenient.

IV. Conclusion

In this letter, we have demonstrated a new type of handheld OCT scanner and a system that can be used at the point-of-care in the clinical primary care environment where both space and time during a patient visit and exam are limited. Experimental results show that our handheld OCT scanner and system have great potential for use in the primary adult and pediatric care offices. Our device provides not only fast 2-D imaging without motion artifacts, but also high resolution 3-D imaging. However, the current imaging speed of our device is not sufficient for full 3-D *in vivo* imaging in the clinic. To enable this, we are currently developing fast signal processing algorithms using graphical processing units. A fully developed and ergonomically engineered handheld probe with a more compact OCT unit would find numerous applications where point-of-care OCT can be applied and potentially used for screening, detecting, diagnosing, and monitoring disease. The ability to utilize more advanced imaging technology in the primary care clinic, particularly by advancing the diagnostic capabilities of otoscopes and ophthalmoscopes, is likely to improve a physician's diagnostic ability, to collect quantifiable data, and to make a more informed decision on patient referral. These advantages have the potential to improve not only the quality of healthcare, but also to reduce costs.

Acknowledgment

The authors would like to thank C. Nguyen for her technical assistance, and Dr. M. Novak and Dr. S. Sayegh for their helpful medical discussions.

References

[1] D. Huang, E. A. Swanson, C. P. Lin, J. S. Schuman, W. G. Stinson, W. Chang, M. R. Hee, T. Flotte, K. Gregory, C. A. Puliafito, and J. G. Fujimoto, "Optical coherence tomography," *Science*, vol. 254, pp. 1178–1181, 1991.

[2] D. C. Adler, Y. Chen, R. Huber, J. Schmitt, J. Connolly, and J. G. Fujimoto, "Three-dimensional endomicroscopy using optical coherence tomography," *Nat. Photon.*, vol. 1, pp. 709–716, 2007.

[3] W. Jung, D. T. McCormick, Y. C. Ahn, A. Sepehr,B. Wong, M. Brenner, N. C. Tien, and Z. Chen, "*In vivo* three-dimensional spectral domain endoscopic optical coherence tomography using a microelectromechanical system mirror," *Opt. Lett.*, vol. 32, pp. 3239–3241, 2007.

[4] S. A. Boppart, B. E. Bouma, C. Pitris, G. J. Tearney, J. F. Southern, M. E. Brezinski, and J. G. Fujimoto, "Intraoperative assessment of microsurgery with three-dimensional optical coherence tomography," *Radiology*, vol. 208, pp. 81–86, 1998.

[5] S. Han, M. V. Sarinko, J. Wu, M. Humayun, and C. Yang, "Handheld forward-imaging needle endoscope for ophthalmic optical coherence tomography inspection," *J. Biomed. Opt.*, vol. 13, pp. 020505-1–020505-3, 2008.

[6] S. A. Boppart, B. E. Bouma, C. Pitris, G. J. Tearney, J. G. Fujimoto, and M. E. Brezinski, "Forward-imaging instruments for optical coherence tomography," *Opt. Lett.*, vol. 22, pp. 1618–1620, 1976.

[7] Y. T. Pan, Z. G. Li, T. Q. Xie, and C. R. Chu, "Hand-held arthroscopic optical coherence tomography for *in vivo* high-resolution imaging of articular cartilage," *J. Biomed. Opt.*, vol. 8, pp. 648–654, 2008.

[8] B. Považay, B. Hofer, C. Torti, B. Hermann, A. R. Tumlinson, M. Esmaeelpour, C. A. Egan, A. C. Bird, and W. Drexler, "Impact of enhanced resolution, speed and penetration on three-dimensional retinal optical coherence tomography," *Opt. Exp.*, vol. 17, pp. 4134–4150, 2009.

[9] I. Grulkowski, M. Gora, M. Szkulmowski, I. Gorczynska, D. Szlag, S. Marcos, A. Kowalczyk, and M. Wojtkowski, "Anterior segment imaging with spectral OCT system using a high-speed CMOS camera," *Opt. Exp.*, vol. 17, pp. 4842–4858, 2009.

[10] R. Steiner, K. Kunzi-Rapp, and K. Scharffetter-Kochanek, "Optical coherence tomography: Clinical applications in dermatology," *Med. Laser Appl.*, vol. 18, pp. 249–259, 2003.

[11] J. M. Ridgway, W. B. Armstrong, S. Guo, U. Mahmood, J. Su, R. P. Jackson, T. Shibuya, R. L. Crumley, M. Gu, and Z. Chen, "*In vivo* optical coherence tomography of the human oral cavity and oropharynx," *Arch. Otolaryngol. Head Neck Surg.*, vol. 132, pp. 1074–1081, 2006.

[12] W. Jung, J. Zhang, J. Chung, P. Wilder-Smith, M. Brenner, J. S. Nelson, and Z. Chen, "Advances in oral cancer detection using optical coherence tomography," *IEEE J. Select. Topics Quantum Electron.*, vol. 11, no. 4, pp. 811–817, Jul./Aug. 2005.

[13] Z. Hu and A. M. Rollins, "Fourier domain optical coherence tomography with a linear-in-wavenumber spectrometer," *Opt. Lett.*, vol. 32, pp. 3525–3527, 2007.

[14] T. Bajraszewski, M. Wojtkowski, M. Szkulmowski, A. Szkulmowska, R. Huber, and A. Kowalczyk, "Improved spectral optical coherence tomography using optical frequency comb," *Opt. Exp.*, vol. 16, pp. 4163–4176, 2008.

[15] M. Mujat, B. H. Park, B. Cense, T. C. Chen, and J. F. de Boer, "Autocalibration of spectral-domain optical coherence tomography spectrometers for *in vivo* quantitative retinal nerve fiber layer birefringence determination," *J. Biomed. Opt.*, vol. 12, pp. 041205-1–041205-6, 2007.

[16] D. L. Marks, A. L. Oldenburg, J. J. Reynolds, and S. A. Boppart, "Autofocus algorithm for dispersion correction in optical coherence tomography," *Appl. Opt.*, vol. 42, pp. 3038–3046, 2003.

[17] N. M. Bressler, A. R. Edwards, A. N. Antoszyk, R. W. Beck, D. J. Browning, A. P. Ciardella, R. P. Danis, M. J. Elman, S. M. Friedman, A. R. Glassman, J. G. Gross, H. K. Li, T. J. Murtha, T. W. Stone, and J. K. Sun, "Retinal thickness on stratus optical coherence tomography in people with diabetes and minimal or no diabetic retinopathy," *Amer. J. Ophthalmol.*, vol. 145, pp. 894–901, 2008.

[18] V. R. Korde, G. T. Bonnema, W. Xu, C. Krishnamurthy, J. Ranger-Moore, K. Saboda, L. D. Slayton, S. J. Salasche, J. A. Warneke, D. S. Alberts, and J. K. Barton, "Using optical coherence tomography to evaluate skin sun damage and precancer," *Lasers Surg. Med.*, vol. 39, pp. 687–695, 2007.

[19] C. C. Yang, M. T. Tsai, H. C. Lee, C. K. Lee, C. H. Yu, H. M. Chen, C. P. Chiang, C. C. Chang, Y. M. Wang, and C. C. Yang, "Effective indicators for diagnosis of oral cancer using optical coherence tomography," *Opt. Exp.*, vol. 16, pp. 15847–15862, 2008.